ISSN 1063-7710, Acoustical Physics, 2017, Vol. 63, No. 5, pp. 583–589. © Pleiades Publishing, Ltd., 2017.
Original Russian Text © S.A. Titov, R.G. Maev, A.N. Bogachenkov, 2017, published in Akusticheskii Zhurnal, 2017, Vol. 63, No. 5, pp. 546–552.

ACOUSTIC SIGNAL PROCESSING. COMPUTER SIMULATION

Lens Multielement Acoustic Microscope in the Mode for Measuring the Parameters of Layered Objects

S. A. Titov[a], *, R. G. Maev[a], and A. N. Bogachenkov[b]

[a] *Institute of Biochemical Physics n.a. N. M. Emanuel, Russian Academy of Sciences, ul. Kosygina 4, Moscow, 119334 Russia*

[b] *Moscow Technological University (MIREA), pr. Vernadskogo 78, Moscow, 119434 Russia*

**e-mail: sergetitov@mail.ru*

Received July 11, 2016

Abstract—An acoustic microscope with a cylindrical lens and ultrasound transducer have been considered, as well as the method based on it for the measuring of longitudinal and transverse wave velocities, the thickness and density of the investigated layer. A theoretical model of the microscope has been constructed, and the relation between the spatiotemporal output signal of the transducer and the angular dependence of the sample reflection coefficient has been found. It has been shown that the velocities of body waves and the thickness can be determined by the delays of ultrasound responses reflected from the layer boundaries measured by the transducer elements, and the density, by the amplitudes of these responses. The method was tested experimentally using a 20-element transducer with a central frequency of 15 MHz and a period of 0.8 mm. The example of a duralumin plate has shown that the error in measuring the thickness and velocity of longitudinal waves error does not exceed 1%; the velocity of transverse waves, 2%; and the density can be estimated with an accuracy of about 5%.

Keywords: acoustic microscope, ultrasound transducer, velocity of volumetric waves, reflection coefficient

DOI: 10.1134/S1063771017050128

1. INTRODUCTION

A scanning acoustic microscope is designed to study the structures of various objects using focused high-frequency ultrasound waves. Single piezoelectric element *1* located coaxially to acoustic lens *2* (Fig. 1a) and operating in echo pulse mode is the most common scheme for a confocal microscope [1]. Mechanical scanning with respect to the object under study *3* is done to construct ultrasound images of the internal structure [2, 3]. The acoustic microscope is also used for to quantitatively characterize local, laterally homogeneous regions of objects by measuring the parameters of flowing surface waves [4, 5], body wave velocities, and layer thicknesses [6, 7]. These quantitative measurement methods are based on the microscope's spatiotemporal signal recorded as a function of displacement of the sample from the focal plane. However, additional mechanical displacement leads to low productivity and requires precision mechanical devices.

The use of multielement ultrasound transducers to measure the acoustic parameters of layered objects makes it possible to replace mechanical scanning with electronic [8, 9]. In such devices, it is possible to record ultrasound responses reflected by the boundaries of the studied layer at different angles and determine the layer parameters from the obtained angular dependences. The element size should be comparable to the wavelength to ensure the required beamwidth and a sufficient spatial sampling rate of the recorded reflected waves. However, fabrication of ultrasound transducers that can operate at the characteristic acoustic microscopy frequencies causes a number of technological difficulties.

A microscope with a spherical acoustic lens and a two-dimensional transducer was proposed recently, the element dimensions of which significantly exceed the wavelength [10]. In such a scheme, the ultrasound beams emitted by the transducer elements are reduced by the lens in the focal region, which allows electronic focusing and scanning in the longitudinal and transverse directions in the natural focal area of the lens, as well as compensation for aberrations.

In this article, a lens multielement microscope with a linear transducer and a cylindrical acoustic lens was proposed and a method was developed for measuring body wave velocities and the thickness and density of a layer.

2. THEORETICAL CONSIDERATION OF THE TECHNIQUE

Figure 1b shows a diagram of the multielement lens microscope. Linear ultrasound transducer with identi-

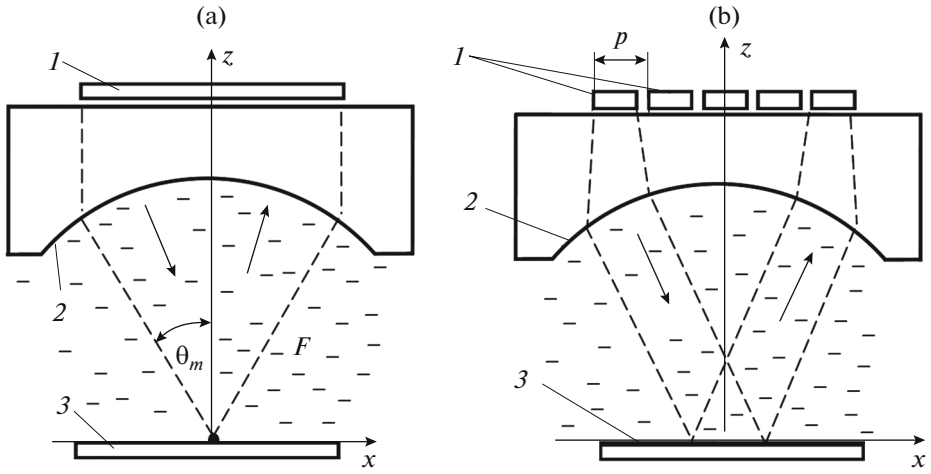

Fig. 1. One-element (a) and multielement (b) acoustic microscopes: (*1*) piezoelements; (*2*) acoustic lens; (*3*) sample.

cal rectangular elements *1* is located in the posterior focal plane of acoustic cylindrical lens *2* at the end of the sound line. The front and back focal distances of the lens are, respectively [11],

$$F = R\frac{C_D}{C_D - C}, \quad F_D = F\frac{C}{C_D}, \tag{1}$$

where R is the lens radius, and C and C_D are the ultrasound velocities in the immersion medium and the lens material, respectively. The propagation of waves from the transducer elements to the sample and back should be considered in order to find the relation between the spatiotemporal output signal of the transducer and the investigated layer parameters. If the transducer element length along the y axis significantly exceeds the characteristic wavelength, the two-dimensional model can be used.

The transducer element being excited by a harmonic signal generates field distribution $u_1(x)$ in the transducer plane. Then the field distribution in the lens plane can be found by convolution in the spatial coordinate of this field with the pulse response of the acoustic line $g_D(x)$ [12]. This response in the Fresnel approximation for the two-dimensional case with an accuracy to an insignificant constant multiplier is [13]

$$g_D(x) = \frac{1}{\sqrt{\lambda_D F_D}}\exp\left(i\frac{2\pi}{\lambda_D}F_D + i\frac{2\pi}{2\lambda_D F_D}x^2\right), \tag{2}$$

where λ_D is the wavelength in the material of the acoustic line. The lens effect on the propagating wave can be taken into account in the paraxial approximation in terms of the phase factor:

$$g_t(x) = \exp\left(-i\frac{k_0 x^2}{2F}\right), \tag{3}$$

where $k_0 = 2\pi/\lambda$, λ is the wavelength in the immersion fluid. Wave propagation in the fluid to the front focal plane ($z = 0$) is described as in (2) by the pulse response:

$$g_W(x) = \frac{1}{\sqrt{\lambda F}}\exp\left(ik_0 F + i\frac{k_0}{2F}x^2\right). \tag{4}$$

Thus, the field in the focal plane can be represented in the form

$$u_f(x) = \{[u_1(x) * g_L(x)]g_t(x)\} * g_W(x), \tag{5}$$

where * denotes the convolution operation. Substituting (2)–(4) into (5) makes it possible to express the field in the front focal plane $u_f(x)$ via the Fourier transformation of the field distribution in the rear focal plane $U_1(k_x) = \mathcal{F}\{u_1(x)\}$:

$$u_f(x) = \frac{1}{\sqrt{\lambda F}}\exp\left(ik_0 F\left(1 + \frac{C^2}{C_D^2}\right)\right)U_1\left(k_0\frac{x}{F}\right). \tag{6}$$

This expression shows that the spectral component of the probing wave with spatial frequency k_x is focused by the lens at the point $x = Fk_x/k_0$. The exponential multiplier determines the phase delay that is common to all the components of the wave spatial spectrum. Formula (6) is an expression of the known lens property to implement the Fourier transformation [12, 13].

The incident field spectral density in the focal plane is determined correspondingly by the field distribution in the transducer plane:

$$u_F(k_x) = \sqrt{\lambda F}\exp\left(ik_0 F\left(1 + \frac{C^2}{C_D^2}\right)\right)u_1\left(-\frac{F}{k_0}k_x\right). \tag{7}$$

Thus, the infinite thin element of the transducer located at point x gives a plane wave incident on the plane at angle $\sin\theta = k_x k_0^{-1} = -xF^{-1}$.

The spectrum of the reflected wave can be obtained by multiplying the spectrum (7) by the reflection coefficient $R(k_x)$ of the sample with respect to the focal

plane. The field distribution of the reflected wave in the transducer plane $u_R(x)$ can be found from the spectral density in the focal plane $U_F(k_x)$ in accordance with a ratio similar to (6):

$$u_R(x) = \exp\left(i2k_0F\left(1+\frac{C^2}{C_D^2}\right)\right)R\left(k_0\frac{x}{F}\right)u_1(-x). \quad (8)$$

Thus, the field value it takes at point x is proportional to the reflection coefficient at $k_x = k_0xF^{-1}$. In order to find the spatiotemporal signal of the transducer under pulsed excitation, inverse Fourier transform of the harmonic components (8) is necessary. Since $k_0 = \omega C^{-1}$, the phase in the exponential multiplier is proportional to frequency ω. Thus, it ensures a constant signal delay and can be omitted from further consideration.

Considering the time dependence of the emitted wave and performing inverse Fourier transformation, the obtained field can be represented as convolution in time:

$$u_R(x,t) = r(x,t) * u_1(-x,t), \quad (9)$$

where

$$r(x,t) = \mathcal{F}_\omega^{-1}\left\{R\left(k_0\frac{x}{F},\omega\right)\right\}. \quad (10)$$

If the reflected wave is received by the converter with the pulse response $u_r(x, t)$, then the output is expressed by the integral of the superposition with respect to the spatial coordinate:

$$s(t) = \int_{-\infty}^{\infty}[r(x,t) * u_t(-x,t)] * u_r(x,t)\,dx. \quad (11)$$

In the proposed measurement method, the emission and reception of the signal are carried out by pairs of transducer elements positioned symmetrically relatively to the axis. If $h_t(x, t)$ and $h_r(x, t)$ are the element characteristics for emitting and receiving respectively, then for the elements whose centers have coordinates $(-x)$ and x, it can be written

$$u_t(\xi,t) = h_t(\xi + x,t), \quad u_r(\xi,t) = h_r(\xi - x,t). \quad (12)$$

Substituting (12) into (11) gives for the output spatiotemporal signal the following expression

$$s(x,t) = \int_{-\infty}^{\infty}[r(\xi,t) * h_t(x-\xi,t)] * u_r(\xi - x,t)\,d\xi. \quad (13)$$

Here the limits of integration are specified as infinite; however, the characteristics of the elements have significant values in the interval $|\xi| < p/2$, where p is the transducer period (Fig. 1b). Determining the total pulse response of the device in the form

$$h(\xi,t) = \int_{-\infty}^{\infty}[h_t(\xi,\tau)h_r(-\xi,t-\tau)]\,d\tau, \quad (14)$$

the output signal is represented as convolution for the spatial and temporal variables of the function of the sample and pulse response:

$$s(x,t) = r(x,t) *^{(t)} *^{(x)} h(x,t). \quad (15)$$

Thus, the result is smoothed over the spatial coordinate, and the width of the pulse response, which is approximately equal to the transducer period p, determines the angular resolution. However, given that the reflection coefficient changes relatively slowly within the angular aperture and p is small compared to the total transducer length, it can assumed that $h(x, t) \approx \delta(x)h_0(t)$ and the following approximation can be used:

$$s(x,t) = r(x,t) * h_0(t). \quad (16)$$

Suppose also that the duration of the ultrasound pulses is less than the time of wave propagation through the layer. Then, in the output signal, the responses reflected from the layer boundaries can be split and the reflection coefficient can be represented as the sum

$$R(k_x,\omega) = \exp\left(-2iz\sqrt{k_0^2 - k_x^2}\right) \times (R_0 + R_L + R_{LT} + R_T \ldots). \quad (17)$$

The exponential multiplier determines the change of the phase of the plane harmonic wave when propagating from the focal plane to the transducer upper boundary and back [14], where coordinate z specifies the position of this boundary. Quantity R_0 is the coefficient of reflection from the interface between the fluid and the layer material. For probing waves to efficiently penetrate the object, the maximum aperture angle is usually selected less than the critical angle for longitudinal waves; therefore, R_0 can be considered a real value depending only on the angle of incidence. Thus, the component of the spatiotemporal signal corresponding to reflection from the surface is equal

$$s_0(x,t) = R_0\left(\frac{x}{F}\right)\delta(t-\tau_W) * h_0(t), \quad (18)$$

where δ is the delta function ensuring a response delay in the liquid by

$$\tau_W = -\frac{2z}{C}\sqrt{1-\left(\frac{x}{F}\right)^2}. \quad (19)$$

The term R_L corresponds to a longitudinal wave which passed through the layer:

$$R_L = T_L\left(\frac{x}{F}\right)\exp\left(2id\sqrt{\omega^2C_L^{-2} - k_x^2}\right). \quad (20)$$

Its amplitude T_L, which is equal to the transmission coefficient through the upper boundary multiplied by the coefficient of reflection from the layer lower boundary, also does not depend on frequency. The corresponding signal component is

$$s_L(x,t) = T_L\left(\frac{x}{F}\right)\delta(t-\tau_W) * \delta(t-\tau_L) * h_0(t), \quad (21)$$

where the additional delay s_L with respect to the pulse s_0 depends on layer thickness d and velocity C_L:

$$\tau_L = \frac{2d}{C_L}\sqrt{1-\left(\frac{C_L x}{CF}\right)^2}. \quad (22)$$

Thus, measuring the delay τ_L for signals from all transducer elements and knowing the velocity of sound in fluid C and the focal length F, it is possible to find d and C_L using model equations (22). The same can be done for the R_T component of the total reflection coefficient (17). This component is formed by the transverse waves in the layer, and the corresponding pulse delay τ_L is determined similarly by (22) with replacement of C_L by the transverse wave velocity C_T. However, the response amplitude of the transverse wave is usually small, especially at small angles of incidence. The response of the mixed mode R_{LT} formed by the longitudinal and transverse waves propagating through the layer in opposite directions is more notable. The delay of the response with respect to the pulse s_0 is

$$\tau_{LT} = (\tau_L + \tau_T)/2, \quad (23)$$

and if we measure this knowing τ_L and d, we can determine the transverse wave velocity C_T. In addition, the ratio of signal amplitudes s_L and s_0 is equal to the ratio of coefficients T_L/R_0, which depend not only on the velocities but on the densities of the fluid and layer material. Thus, knowing the velocity values determined in the previous stage of processing, and the liquid density, we can find the layer density.

The range of applicability of the method is limited by the approximation introduced above (16), based on the slowness of change in the object function $r(x, t)$ over the aperture of an individual transducer element. Since the amplitude coefficients R_0 and T_L are smooth, delays (19) or (22) make the main contribution to the change in rate of r . Thus, variation of the delay within the transducer period p should be less than the ultrasound period:

$$\left|\frac{d\tau}{dx}\right| p < \frac{\lambda}{C}. \quad (24)$$

Substitution of (19) and (22) into (24) gives, respectively,

$$zp < \frac{\lambda F}{2\sin\theta_m}, \quad dp < \frac{C\lambda F}{2C_L\sin\theta_m}, \quad (25)$$

where θ_m is the maximum angle of aperture (Fig. 1) whose sine is the ratio of the maximum x to the focal length F. At typical values of $\theta_m \approx 0.2$, $C_L = 4C$, and $p = 10\lambda$, the defocusing z and layer thickness d should not exceed $z < F/4$, $d < F/16$.

3. EXPERIMENTAL

The method was experimentally with an ultrasound transducer of $N = 20$ rectangular elements. The transducer period was $p = 0.8$ mm, and the long side of the element was 1.2 mm. The central frequency of the element's frequency characteristic in the transmitting–receiving mode and the relative band at a 6 dB level was 15 MHz and 60%, respectively. A cylindrical acoustic lens made of polystyrene with a radius $R = 13$ mm, the axis of which was oriented along the long side of the transducer elements, was attached to the grid. Water was used as the immersion liquid, which on the basis of (1) gives a focal length of $F = 35$ mm. The distance between the lens and the transducer was 17 mm, which is close to the back focal length of $F_D = 22$ mm. The width of the ultrasound transducer was $Np = 16$ mm, which ensured the maximum aperture angle $\theta_m = 12°$.

Sequential pulse excitation of the transducer elements with numbers k ($k = 1, ..., N$) and element signal recording with numbers $N - k + 1$, arranged with respect to the lens axis symmetrically to the radiating elements was carried out to generate an output spatio-temporal signal using a multichannel electronic unit. Thus, the coordinate of the transmitting transducer element is $x = 0.5(2k - N - 1)p$. The signal $s_k(t)$, measured for the duralumin plate with a thickness $d = 3.21 \pm 0.01$ mm is shown in the form of a halftone chart in Fig. 2. The sample was vertically displaced towards the lens, so that its upper surface was in the position $z \approx 16.5$ mm. The above-mentioned components s_0, s_L, the response of the longitudinal-transverse mode s_{LT}, and the response s_{L2} formed by the wave double passage through the layer are observed in the received signal. The signal component formed by the transverse wave is weak and not detected in the image.

The arrival time of the response s_0 reflected from the layer upper boundary is determined by expression (19). As the layer is displaced from the focal plane, this delay varies significantly depending on the position of the receiving–transmitting pair of the transducer elements. The response of the longitudinal waves s_L is delayed with respect to s_0 by the value of τ_L (22). In this experiment, delays τ_L and τ_W have opposite signs and are comparable in magnitude; therefore, the response arrival time depends weakly on k. Not only longitudinal but also transverse waves participate in the formation of the response s_{LT}, so its amplitude is small in the region of small angles of incidence.

In the practical implementation of the method, it should be taken into account that the velocity of sound in the lens material and immersion medium, as well as the lens radius and focal length, are known with some

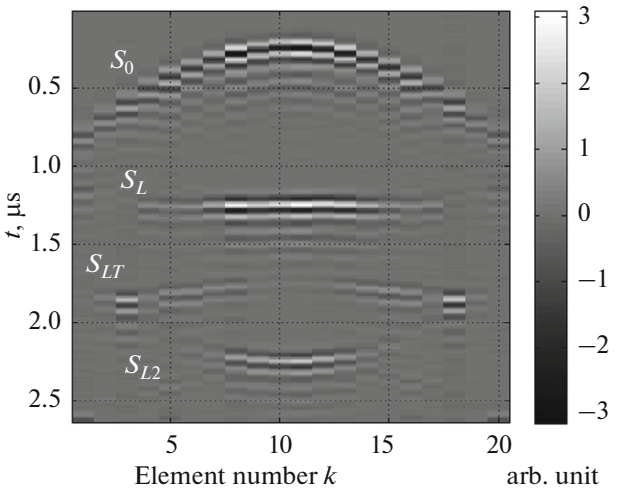

Fig. 2. Transducer signal $s_k(t)$ measured for duralumin plate. Signal amplitude at $t > 1$ μs is increased fourfold.

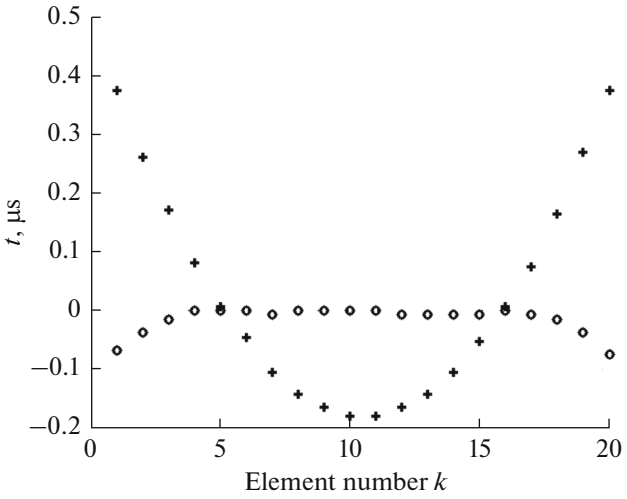

Fig. 3. Delays t_0 (○) and t_1 (+) of signals reflected at position of reflector $z = 0$ and $z = 16.48$ mm, respectively.

errors. In addition, the acoustic lens has aberrations, and the transducer elements can be located with errors with respect to the vertical axis. Therefore, it is advisable to calibrate the instrument for measuring the angles of propagation of the waves emitted and received by the transducer elements. The values $\beta_k = \sin\theta_k$ can be found by measuring the signal relative delays τ_k occurring in the displacement of an ideal plane reflector along the vertical axis Δz. Knowing the velocity of sound in water C and the displacement Δz, the magnitude of β_k can be found from expression (19):

$$\beta_k = \sqrt{1 - \left(\frac{\tau_k C}{2\Delta z}\right)^2}. \qquad (26)$$

Figure 3 shows the times t_0 and t_1 of signal arrivals from the surface of a polished steel sample located approximately in the lens focal plane ($z = 0$) and shifted towards the lens at a distance $\Delta z = 16.48$ mm. The times are measured with respect to the time of arrival t_0 of the signal emitted by the element $k = 10$, and time t_1 is increased on the graph by 22 μs. As follows from the presented data, time t_0 is not constant for all transducer elements. Most notably, this effect manifests itself at the edges of the transducer, which can be explained by the increase in lens aberration with increasing angle of incidence. Figure 4 shows the β_k values determined by the measured delays $\tau_k = t_{0k} - t_{1k}$ in accordance with (26). The figure shows also the results of calculating β_k by the known geometrical parameters of the lens and transducer $\beta_k = x_k F^{-1}$. There are marked differences between the calculated and experimental values, which make it expedient perform calibration.

The relative delays τ_L and τ_{LT} for the investigated duralumin plate were measured after calibration, the results of which are shown in Fig. 5 as a function of parameter β_k. The correlation method was used to determine the pulse delays s_L and s_{LT} with respect to the s_0 pulses and the polarity change of the pulses s_L and s_{LT} reflected from the lower metal–liquid boundary was taken into account. τ_L and β were then averaged for pairs of transmitting transducer elements symmetrically located with numbers k and $N - k + 1$. The squaring of expressions (22) makes it possible to obtain a linear regression equation with the independent variable β_k^2 and dependent variable τ_{Lk}^2, $k = 1, ..., N$:

$$\tau_{Lk}^2 = \frac{4d^2}{C_L^2} - 4d^2\beta_k^2. \qquad (27)$$

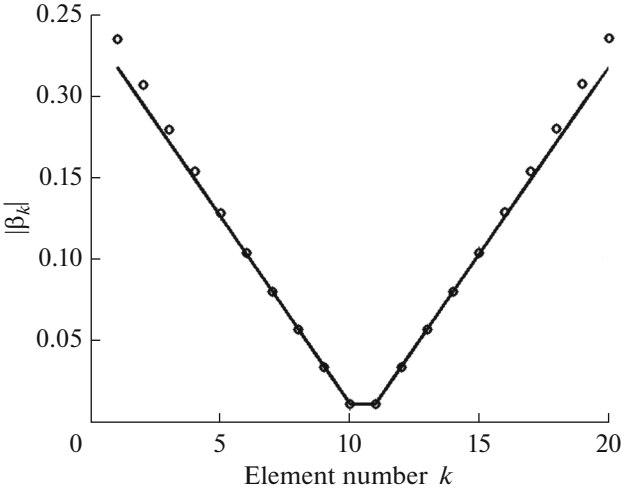

Fig. 4. Parameters β_k: calculation (–) and experiment (○).

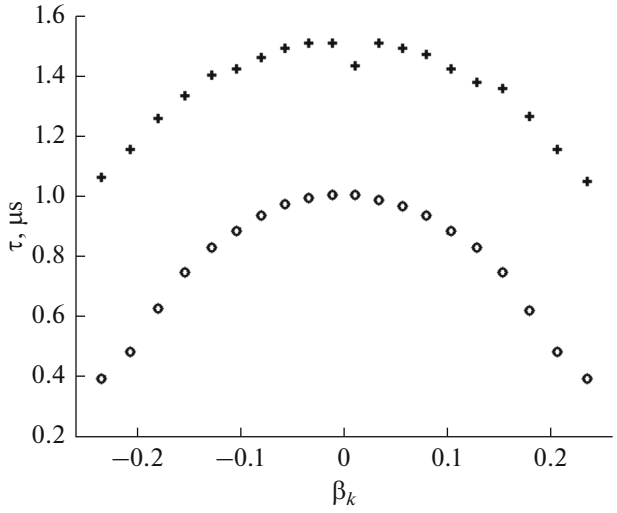

Fig. 5. Delays τ_L (○) and τ_{LT} (+) measured for duralumin plate.

Finding the coefficients of this equation by the least squares method, it is possible to determine d and C_L. Multiple repeat measurements of the sample under consideration give $d = 3.17 \pm 0.03$ mm and $C_L = 6380 \pm 40$ m/s. Similarly, the transverse wave velocity C_T was calculated based on the delay τ_T, which was determined by the measured delays τ_{LT} and τ_L according to (23), because the response amplitude of the longitudinal–transverse mode s_{LT} is significantly smaller than the response amplitude s_L in the region of the small angles of incidence. The calculation was carried out for the limited data interval $2 < k < 9$, and the used thickness value d was determined at the previous processing stage. The resulting value is $C_T = 3120 \pm 50$ m/s. The results of the velocity measurements agree with the published data for duralumin alloy data $C_L = 6300–6400$ m/s and $C_T = 3100–3200$ m/s [15, 16], and the found plate thickness corresponds to the value measured by an independent method ($d = 3.21$ mm). Thus, the relative measurement error does not exceed 1% for d and C_L and 2% for C_T.

The density of the layer material ρ can be found from the recorded signal amplitudes. As follows from expressions (18) and (21), the ratio of the response amplitudes s_L and s_0 does not depend on the characteristics of the microscope and is determined only by the wave reflection and transmission coefficients at the layer boundaries $\gamma = T_L / R_0$. For normal incidence, this coefficient is [14]

$$\gamma = \frac{4ZZ_W}{(Z + Z_W)^2}, \qquad (28)$$

where $Z = \rho C_L$, and Z_W are the impedances of the layer and water, respectively. The measured value of the amplitude ratio was $\gamma = 0.27 \pm 0.01$, which implies a density estimate of $\rho = 2.95 \pm 0.13$ g/cm^3. The relative error in density estimation in this case does not exceed 5%; however, the average value is somewhat overestimated compared to the published values of $\rho = 2.7–2.8$ g/ cm^3. One of the causes of the displacement can be neglect of ultrasound attenuation in the layer material in view of the amplitude ratio (28).

CONCLUSIONS

We have proposed an acoustic microscope with a cylindrical acoustic lens and ultrasound linear transducer located at the back focal plane of the lens; with its use, we have developed a technique for measuring body wave velocities, thickness, and the density of a studied layer. The output spatiotemporal signal of the microscope is formed by pairs of transducer transmitter–receiver elements arranged symmetrically with respect to the acoustic axis. In the paraxial approximation, it is shown that the signal is determined by the coefficient of wave reflection from the layer surface with the angle of incidence determined by the distance between the transmitter and receiver elements. We have theoretically and experimentally shown that the desired layer parameters can be found from the angular dependences of the amplitudes and delays of the ultrasound responses reflected from the layer boundaries. The measurement technique is demonstrated by the example of an isotropic plate; however, the presence of the cylindrical lens, ensuring the selectivity for the azimuthal angle, makes it possible to use the microscope for studying anisotropic materials. It should also be noted that in this microscope scheme, the sizes of elements can significantly exceed the characteristic wavelength, which simplifies manufacture of the transducer for the high-frequency range.

ACKNOWLEDGMENTS

The study was supported by the Russian Foundation for Basic Research (project no. 16-07-01236).

REFERENCES

1. *Advances in Acoustic Microscopy and High Resolution Imaging: From Principles to Applications,* Ed. by R. Maev, (Wiley-VCH, Weinheim, Germany, 2013).
2. Bing-Feng Ju, Xiaolong Bai, and Jian Chen, Rev. Sci. Inst. **83** (3), 035113 (2012).
3. Yu. S. Petronyuk, E. S.Morokov, and V. M. Levin, Bull. Russ. Acad. Sci.: Phys. **79** (10), 1268–1273 (2015).
4. J. Kushibiki, Y. Ono, Y. Ohashi, and M. Arakawa, IEEE Trans. Ultrason., Ferroelectr. Freq. Control. **49** (1), 99–113 (2002).

5. X. D. Deng, T. Monnier, P. Guy, and J. Courbon, J. Appl. Phys. **113** (22), 224508 (2013).
6. H. Volker, J. Appl. Phys. **84** (2), 668–670 (1998).
7. Ch. Jian, B. Xiaolong, Y. Keji, and J. Bing-Feng, Ultrasonics **56**, 505–511 (2015).
8. C. J. L. Lane, A. K. Dunhill, B. W. Drinkwater, and P. D. Wilcox, IEEE Trans. Ultrason., Ferroelectr. Freq. Control. **57** (12), 2742–2752 (2010).
9. S. A. Titov and R. G. Maev, Acoust. Phys. **59** (5), 600–607 (2013).
10. S. A. Titov and R. G. Maev, Tech. Phys. Lett. **42** (9), 447–450 (2016).
11. G. A. D. Briggs and O. V. Kolosov, *Acoustic Microscopy* (Oxford Univ., New York, 2010), 2nd ed.
12. J. W. Goodman, I*ntroduction to Fourier Optics* (McGraw-Hill, New York, 1968).
13. A. Papoulis, *Systems and Transforms with Application in Optics* (Robert Krieger Publishing Company, Malabar, Florida, 1968).
14. L. M. Brekhovskikh and O. A. Godin, Acoustics of Layered Media (Nauka, Moscow, 1989) [in Russian].
15. I. N. Ermolov and I. N. Lange, *Ultrasonic Control* (Mashinstroenie, Moscow, 2004) [in Russian].
16. A. S. Birks, R. E. Green, and P. McIntire, *Ultrasonic Testing. Nondestructive Testing Handbook*. ***Vol. 7*** (Am. Soc. Nondestr. Testing, Columbus, OH, 1991) 2nd ed.

Translated by N. Petrov